Pflugers Arch - Eur J Physiol (2013) 465:945–953
DOI 10.1007/s00424-012-1199-3

ION CHANNELS, RECEPTORS AND TRANSPORTERS

A basic residue in the proximal C-terminus is necessary for efficient activation of the M-channel subunit Kv7.2 by PI(4,5)P_2

Vsevolod Telezhkin · Alison M. Thomas · Stephen C. Harmer Andrew Tinker · David A. Brown

Received: 5 November 2012 / Revised: 3 December 2012 / Accepted: 3 December 2012 / Published online: 6 January 2013

Abstract All Kv7 potassium channels require membrane phosphatidylinositol-4,5-bisphosphate (PI(4,5)P_2) for their normal function and hence can be physiologically regulated by neurotransmitters and hormones that stimulate phosphoinositide hydrolysis. Recent mutational analysis indicates that a cluster of basic residues in the proximal C-terminus (K354/K358/R360/K362) is crucial for PI(4,5)P_2 activation of cardiac Kv7.1 channels. Since this cluster is largely conserved in all Kv7 subunits, we tested whether homologous residues are also required for activation of Kv7.2 (a subunit of neuronal M-channels). We found that the mutation Kv7.2 (R325A) (corresponding to R360 in Kv7.1) reduced Kv7.2 current amplitude by ~60 % ($P<0.02$) without change in voltage sensitivity and reduced the sensitivity of Kv7.2 channels to dioctanoyl-phosphatidylinositol-4,5-bisphosphate by ~eightfold ($P<0.001$). Taking into account previous experiments (Zhang et al., Neuron 37:963–75, 2003) implicating Kv7.2 (H328), and since R325 and H328 are conserved in homologous positions in all other Kv7 channels, we suggest that this proximal C-terminal domain adjacent to the last transmembrane domain that contains R325 and H328 (in Kv7.2) might play a major role in the activation of all members of the Kv7 channel family by PI(4,5)P_2.

Keywords Potassium channels · Phosphatidylinositol-4,5-bisphosphate (PIP_2) · Membrane currents

Abbreviations

diC_8-PI(4,5)P_2	Dioctanoyl-phosphatidylinositol-4,5-bisphosphate
PI(4,5)P_2	Phosphatidylinositol-4,5-bisphosphate
P_{open}	Channel open probability

Introduction

The five members of the family of Kv7 (*KCNQ*) potassium channels form voltage-gated channels that play a major role in regulating cell excitability [11, 17]. Kv7.1 subunits, with their associated KCNE1 proteins, form the cardiac delayed rectifier channel I_{Ks}. Kv7.2 through Kv7.5 are primarily localized to the nervous system, where they form homomeric or heteromeric non-inactivating voltage-gated potassium channels (including the M-channel [23]) that control neural excitability [3]. Kv7.4 and Kv7.5 also control the contractility of smooth muscle cells [7].

All members of this family require the presence of the membrane phospholipid phosphatidylinositol-4,5-bisphosphate (PI(4,5)P_2) for their normal function [6]. PI(4,5)P_2 controls the voltage sensitivity of the cardiac Kv7.1/KCNE1 channel [14], whereas it sets the maximum open probability of Kv7.2-7.5 channels, without apparently altering their voltage dependence [12, 19, 20]. PI(4,5)P_2 dependence is important physiologically because it allows Kv7 channel activity to be altered by transmitters and hormones that stimulate PI(4,5)P_2 hydrolysis and reduce PI(4,5)P_2 levels [5, 6]. Hence, it is helpful to know which component(s) of

V. Telezhkin · D. A. Brown (✉)
Department of Neuroscience, Physiology and Pharmacology, University College London, Gower Street, London WC1E 6BT, UK
e-mail: d.a.brown@ucl.ac.uk

A. M. Thomas · S. C. Harmer · A. Tinker
William Harvey Heart Centre, Barts and The London School of Medicine and Dentistry, Charterhouse Square, London EC1M 6BQ, UK

Present Address:
V. Telezhkin
Cardiff School of Biosciences, The Sir Martin Evans Building, Museum Avenue, Cardiff CF10 3AX, UK

the Kv7 channel protein are responsible for sensing PI(4,5)P_2.

Individual members of the Kv7.2-7.5 subgroup vary over a hundred-fold in their sensitivity to PI(4,5)P_2 as a channel activator [12]. This difference was traced (in part, at least) to variations in a cluster of basic residues (K452/R459/R461in Kv7.2; see Fig. 1) in the linker between helices A and B in the channel C-terminus and hence adduced to be part of the binding site for PI(4,5)P_2 in this subgroup of Kv7 channels [10]. However, this cluster is not present in Kv7.1. Instead, mutational studies have suggested two other groups of basic residues in the Kv7.1 C-terminus as PI(4,5)P_2 activation sites: the more distal residues R539 and R555 (which are naturally mutated in patients with the long QT syndrome [16]) and the cluster K354/K358/R360/K362 at the extreme proximal start of the C-terminus (Fig. 1) [22]. Mutations of these residues to neutral alanines reduced binding of phosphoinositides to a Kv7.1 C-terminal fusion protein and produced a large positive shift in Kv7.1/KCNE1 voltage sensitivity [22].

Since the cluster K354/K358/R360/K362 in Kv7.1 is also strongly represented in other members of the Kv7 family, including Kv7.2 (Fig. 1), we wondered whether mutating the homologous residues in Kv7.2 to alanines might also affect Kv7.2 channel activity and sensitivity to PI(4,5)P_2. We find that one such mutation (R325A) does indeed markedly impair the response of Kv7.2 channels to PI(4,5)P_2. Taken in conjunction with the previous observation [25] that a mutation of the immediately adjacent histidine H328 also reduced Kv7.2 sensitivity to PI(4,5)P_2, and bearing in mind that R325 and H328 in Kv7.2 are conserved among *all* Kv7 channels, we suggest that this region might play a major role in the activation of all Kv7 channels by PI(4,5)P_2.

Methods

Site-directed mutagenesis

The human Kv7.2 channel construct (accession number, AF110020.1), provided by David McKinnon (SUNY, Stony Brook, USA; see [23]) and cloned into pCR3.1 (Invitrogen) was used as the template for mutagenesis. The Quikchange site-directed mutagenesis kit (Agilent Technologies, Santa Clara, CA, USA) was used, as per manufacturer's instructions, to mutate arginine 325 (R325A) and lysine 327 (K327A) to alanine singly, and in combination, within the proximal C-terminal region of Kv7.2. The primer sets employed were (5′–3′): R325A sense: AAGGTTCAGGAGCAGCACGCGCAGAAGCACTTTGAGAAGAGGCGG, R325A antisense: CCGCCTCTTCTCAAAGTGCTTCTGCGCGTGCTGCTCCTGAACCTT, K327A sense: AAGGTTCAGGAGCAGCACAGGCAGGCGCACTTTGAGAAGAGGCGG, K327A antisense: CCGCCTCTTCTCAAAGTGCGCCTGCCTGTGCTGCTCCTGAACCTT, R325A/K327A sense: AAGGTTCAGGAGCAGCACGCGCAGGCGCACTTTGAGAAGAGGCGG, and R325A/K327A antisense: CCGCCTCTTCTCAAAGTGCGCCTGCGCGTGCTGCTCCTGAACCTT. All constructs, and the introduction of mutations, were verified by automated sequencing.

Cell culture and transfection

Methods for cell culture and transfection were as described in [20]. In brief, all experiments were performed on Chinese hamster ovary (CHO) cells stably transfected to express the human muscarinic receptor type 1 (HM1). Cells were transiently co-transfected with 5 μg pCR3.1 plasmid encoding either the wild-type (wt) human Kv7.2 channel or single R325A or K327A mutations or double R325A/K327A mutations (see above), plus a cDNA plasmid encoding the enhanced green fluorescent protein (eGFP) in an eGFP: Kv7.2 cDNA ratio of 1:10. During transfection, HM1-CHO cells were incubated in Opti MEM medium (Invitrogen Inc.) in a humidified incubator gassed with 5 % CO_2/95 % air for 3 h then Opti MEM was replaced with Alpha MEM medium (Invitrogen Inc.) supplemented with 10 % foetal calf serum, 1 % penicillin/streptomycin and 1 % L-glutamine. Transfected cells were then plated onto coverslips and incubated in Alpha MEM medium (Invitrogen Inc.) supplemented with 10 % foetal calf serum, 1 % penicillin/streptomycin and 1 %L-glutamine in a humidified incubator gassed with 5 % CO_2/95 % air. Cells expressing eGFP (assayed by fluorescence microscopy) were used for electrophysiological experiments between 18 and 72 h following transfection.

Electrophysiological recordings

Macroscopic Kv7.2 currents were recorded using the voltage clamp perforated-patch technique as described in [18]. The bath solution contained (in millimolar): 144 NaCl, 2.5 KCl, 0.5 $MgCl_2$, 2 $CaCl_2$, 10 D-glucose, and 5 N-2-hydroxyethylpiperazine-N′-2-ethanesulfonic acid (HEPES); pH was adjusted to 7.4 using Trizma base (TRIS). The pipette solution contained (in millimolar): 30 KCl, 80 K-acetate, 40 HEPES, 3 $MgCl_2$, 1 $CaCl_2$, and 30 ethylene glycol tetraacetic acid (EGTA); free $[Ca^{2+}]_i$ was adjusted to 100 nM; pH was adjusted to 7.2 with KOH. Amphotericin B 300 μg/μL was used as a perforating agent. All experiments were performed at a controlled room temperature (22±0.5 °C).

Single Kv7.2 channel activity was recorded in membrane patches from transfected HM1-CHO cells excised into inside-out configuration as described previously [20]. The pipette solution used was the same as the bath solution used for perforated-patch studies (see above). The bath solution

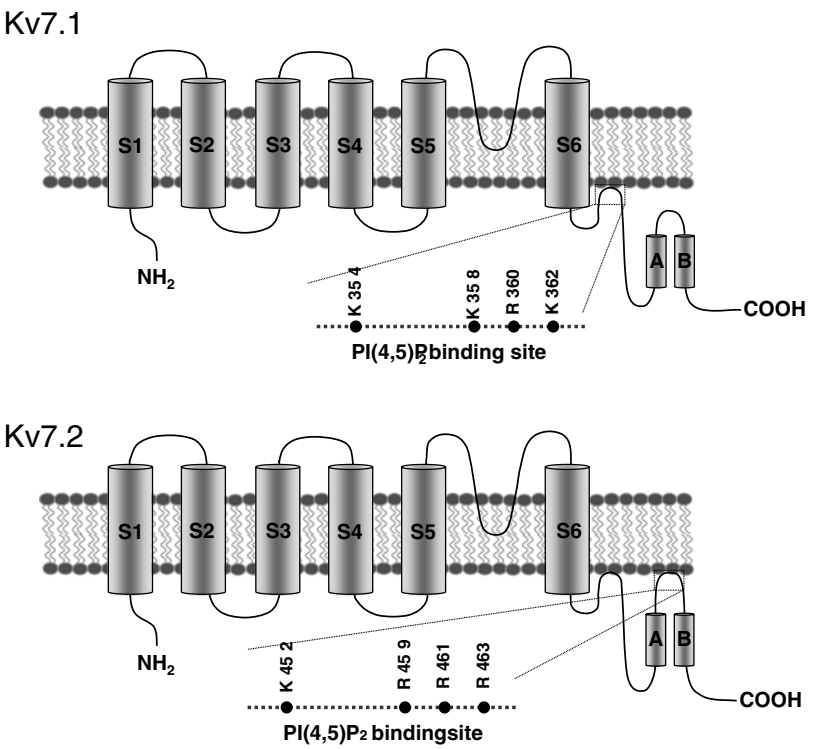

Fig. 1 Diagrammatic representation of Kv7.1 and Kv7.2 potassium channels with some of the residues in the C-terminus previously reported to be involved in channel activation by $PI(4,5)P_2$ as determined by mutational analysis (Kv7.1 (K354/K358/R360/K362): [22]; Kv7.2(H328): [25]; Kv7.2 (K452/R459/R461): [10])

for inside-out studies contained (in millimolar): 165 KCl, 5 HEPES, and 10 EGTA; pH was adjusted to 7.2 using NaOH. Non-hydrolysable ATPγS (0.1 μM) was constantly present in the bath solutions during inside-out studies in order to inhibit endogenous production of $PI(4,5)P_2$ by phosphatidylinositol kinases that might remain associated with the excised patch. To study the effects of $PI(4,5)P_2$ on channel activity, the water-soluble dioctanoyl analogue diC_8-$PI(4,5)P_2$ was applied to the isolated inside-out patches in incremental concentrations from 1 to 300 μM using a fast microperfusion system (delivery time<1 s). The maximum concentration applied was limited to 300 μM for technical reasons.

All electrophysiological studies were performed using an Axopatch 200A amplifier and Digidata 1440 A/D interface (Axon Instruments, Forster City, CA, USA) and pipette holder optimized for low noise recordings (G23 Instruments, UCL). All recordings were filtered with an eight-pole Bessel filter at 5 kHz and digitized at 10 kHz. For recording, macroscopic currents in perforated-patch configuration cells were held at −70 mV and commanded to voltages from −100 to +70 mV in steps of 3 s duration and increments of ±10 mV. Series resistance was compensated 60–90 %. For recording single Kv7.2 channel activity, we used a gap-free protocol at a constant pipette potential of 0 mV. Pipette resistances of both perforated-patch and inside-out configurations were ~5–10 MΩ when filled with the corresponding solutions.

Data analysis

The data were analysed using Clampfit 10.2, Microsoft Office Excel 2003, and Microcal Origin 6.0 software. Current–voltage relationships for the perforated-patch studies were determined using 2–3 s voltage commands between −100 and +70 mV in 10 mV steps from a holding potential of −70 mV and steady-state current densities plotted against command voltage (V_c). Conductances (G) were calculated by dividing current by the

driving force (V_c–E_K), with E_K ~ −95 mV, plotted against command voltage and fitted with a Boltzmann equation using an iterative fitting routine:

$$G/G_{max} = 1/\{1 + \exp(V_{0.5} - V_c)/k\} \quad (1)$$

where G_{max} is the extrapolated maximum conductance, $V_{0.5}$ is the voltage (in millivolt) corresponding to half the maximum conductance, and k is the slope factor (in millivolt).

Single-channel currents were measured and channel P_{open} determined as described in [20]. Channel openings <0.5 ms duration were ignored. Since most of the recordings were made from multi-channel patches containing up to six channels, the number of channels in each patch (N) was determined by fluctuation analysis using the equation:

$$Var(I_m) = Var_{Background} + i_{unit}I_m - \frac{I^2{}_m}{N} \quad (2)$$

where I_m is the mean total current amplitude, $Var(I_m)$ is current variance, and i_{unit} is the single-channel current measured at low diC$_8$-PI(4,5)P$_2$ concentrations from all-point histograms. Patch NP_{open} was then corrected for this estimate of N. Data were collected over the last 20 s of exposure to each concentration of diC$_8$-PI(4,5)P$_2$, when NP_{open} was stable, and deduced single-channel P_{open} plotted against diC$_8$-PI(4,5)P$_2$ concentration ($[PIP_2]$) by applying the following single-site Hill equation with a least-squares plotting routine:

$$P_{open} = P_{open(max)}/\left\{1 + [EC_{50}/[PIP_2]]^{nH}\right\} \quad (3)$$

where $P_{open(max)}$ is the maximum extrapolated single-channel P_{open}, EC_{50} is the concentration of diC$_8$-PI(4,5)P$_2$ producing half $P_{open(max)}$ and nH is the Hill slope. Curves were constrained to $P_{open(max)} \leq 1$; no other constraints were imposed.

Equations (1) and (3) were first fitted to the data generated from individual whole cell or isolated patch experiments, respectively, the appropriate set of parameters obtained, and then averaged to give the mean values (±SEM) shown in Tables 1 and 2 below. These latter values were then used to construct the curves shown in Figs. 2 and 4. Statistical comparisons of means were performed using one-way ANOVA; differences were considered significant at $P<0.05$.

Table 1 Currents generated by transfecting HM1-CHO cells with wild-type or mutated Kv7.2 cDNAs

Mutation	Current density at +70 mV (pA/pF)	G/G_{max} $V_{0.5}$ (mV)	G/G_{max} slope factor k
Kv7.2 wild type (n=11)	40.2±5.4	−14.6±4.1	21.7±2.6
K327A (n=8)	47.3±8.6	−18.4±3.7	21.6±1.9
R325A (n=7)	16.4±6.1*	−11.7±6.6	22.9±3.6
R325A/K327A (n=11)	6.4±1.6**	−10.7±7.1	22.4±2.4

*$P<0.02$, **$P<0.001$, significantly different from wild-type Kv7.2

Western blots

HM1-CHO cells were transfected in 10 cm dishes using Turbofect (Fermentas) with 5 μg pCR3.1-Kv7.2 wild type or mutant plasmids and 100 ng of eGFP. After 48 h, cells were washed twice with ice-cold phosphate-buffered saline (PBS) and harvested by scraping them from the surface. The cells were pelleted at 1,000×g for 4 min and resuspended in 1:1 mixture of PBS and sodium dodecyl sulphate (SDS) loading buffer. Cells were sonicated and denatured at 70 °C for 20 min before loading samples onto SDS PAGE. Western blotting was carried out using standard techniques. Kv7.2 protein was detected using a goat anti-Kv7.2 N-terminal antibody (1:500 dilution, sc-7793, Santa Cruz Biotechnology, USA) followed by a horseradish peroxidase (HRP)-conjugated rabbit anti-goat secondary antibody (1:5,000 dilution, A5420, Sigma-Aldrich, UK). To determine the total amount of protein loaded, a rabbit anti-heat shock protein (HSP)-90 antibody (1:1,000 dilution, sc-7947, Santa Cruz Biotechnology, USA) followed by an HRP-conjugated goat anti-rabbit secondary antibody (1:10,000 dilution, sc-2054, Santa Cruz Biotechnology, USA) was used. Detection was carried out using ECL detection reagents (GE Healthcare, UK).

Chemicals

All compounds for solutions, including amphotericin B and adenosine 5′-O-(3-thiotriphosphate) (ATPγS), were purchased from Sigma-Aldrich; diC$_8$-PI(4,5)P$_2$ was purchased from Echelon Inc.

Results

Macroscopic currents: perforated-patch recording

When depolarized for 2–3 s from a holding potential of −70 mV, HM1-CHO cells that had been transiently transfected with cDNA plasmids encoding the wild-type Kv7.2 channel (wt-Kv7.2) expressed large time- and voltage-dependent outward currents, with a current density of 40.2±5.4 pA pF^{-1} (n=11) at +70 mV and a threshold between −60 and −50 mV, as previously reported [18] (Fig. 2a, b and Table 1). Leak currents with hyperpolarizing steps down to −100 mV were negligible (≤1 pA pF^{-1}). Calculated conductance–voltage curves (Fig. 2c) yielded a half-maximal activation voltage ($V_{0.5}$) of −14.6±4.1 mV and slope factor (k) of 21.7±2.6 mV (Table 1; cf. 13.8 and 12.1 mV, respectively, in [18]).

We then tested the effect of expressing cDNAs for the mutated Kv7 channels Kv7 (R325A) and Kv7 (K327A), singly and in combination. These mutations correspond to the R360A and K362A mutations of Kv7.1 which reduced Kv7.1/KCNE1

Table 2 Effect of diC_8-PI(4,5)P_2 on the activity of wild-type and mutated Kv7.2 channels recorded in excised inside-out membrane patches

Mutation	Single-channel current (pA)	P_{open} at 300 μM diC_8-PI(4,5)P_2	Extrapolated $P_{open(max)}$	diC_8-PI(4,5)P_2 EC_{50} (μM)	diC_8-PI(4,5)P_2 Hill slope *nH*
Kv7.2 wild type (*n*=10)	0.54±0.011	0.73±0.072	0.87±0.059	120.3±32.43	2.08±0.348
K327A (*n*=10)	0.57±0.013	0.69±0.067	0.81±0.075	114.6±20.55	1.06±0.111*
R325A (*n*=8)	0.51±0.012	0.29±0.110**	0.85±0.081	980±132***	1.33±0.230
R325A/K327A (*n*=8)	0.55±0.015	0.18±0.067***	0.84±0.113	982±200***	1.75±0.234

*P<0.01, **P<0.004, ***P<0.001, significantly different from the wild-type Kv7.2

current densities at +40 mV by ~70 % [22]. We did not test K321A because the corresponding mutation of Kv7.1 (K354A) had a relatively small effect on Kv7.1/KCNE1 currents [22]; the other mutation-sensitive residue in Kv7.1 (K358) is already replaced by glutamine (Q) in Kv7.2 (see Fig. 1).

The K327A mutation had no significant effect on Kv7.2 currents: neither current densities nor conductance $V_{0.5}$ values obtained on expressing the Kv7.2 (K327A) channel were significantly different from Kv7.2-wt (Fig. 2b, c). In contrast, the R325A mutation, and the double-mutant R325A/K327A, strikingly reduced current densities at +70 mV by ~60 %, to 16.4±6.1 $pA pF^{-1}$ (P<0.02), and by ~84 %, to 6.4±1.6 pA pF^{-1} (P<0.001), respectively; mean R325A and R325A/K327A current amplitudes were not significantly different (P<0.076). Interestingly, this reduction of current amplitude was not accompanied by any apparent change in voltage sensitivity, as judged from the conductance $V_{0.5}$ (Fig. 2c and Table 1).

We were concerned that the changes in current amplitudes seen with these mutations might have arisen from reduced channel protein expression. There was no change

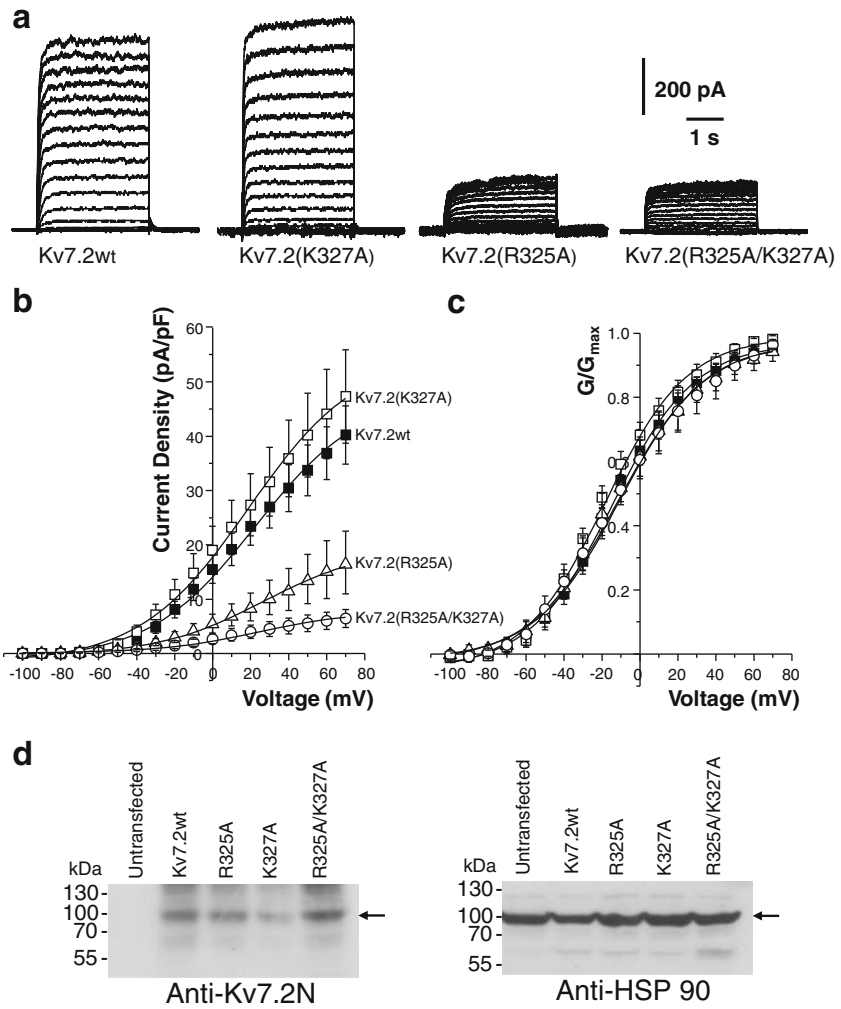

Fig. 2 Currents in HM1-CHO cells transfected with cDNA plasmids encoding wild-type (wt) and mutated Kv7.2 channels. Cell-attached perforated-patch recording. **a** Currents generated by 3 s voltage steps from −100 to +70 mV in incremental steps of 10 mV from a holding potential of −70 mV. **b** Mean current densities (in picoampere per picofarad) plotted against command potential (in millivolt). *Bars* show SEMs (*n*=7–11 for each mutant). **c** Plots of fractional conductance (G/G_{max}) against command voltage. Curves are least-squares Boltzmann plots of mean current **b** and conductance **c** against command voltage (see 'Methods' section, Eq. (1)). Mean values for the parameters used are given in Table 1. **d** Western blots showing the total expression of wild-type or mutant proteins within transfected HM1-CHO cells. Kv7.2 was detected as a 100-kDa band (*left hand panel*) and the total amount of protein loaded was confirmed to be similar by detection of the molecular chaperone, HSP-90 (*right hand panel*). The marker shown is the Page Ruler Prestained protein ladder (Fermentas, UK)

in total protein expression, as judged from Western blots (Fig. 2d). Although this does not exclude a change in plasma membrane expression, single-channel recordings (see below) suggest this not to be an important factor since the reduced macroscopic current amplitudes were matched by reduced openings of the individual channels.

Single-channel properties: isolated inside-out patch recording

Kv7.2-wt channel activity identified in on-cell recording rapidly dissipated on patch excision in inside-out mode into the ATPγS-containing 'intracellular' solution, presumably due to loss of PI(4,5)P_2 from the isolated membrane patch (see [20]). Activity could then be generated by adding incremental concentrations of diC$_8$-PI(4,5)P_2 to the inside face of the membrane patch (Fig. 3a). When corrected for the number of channels (see 'Methods' section), the maximum observed single-channel open probability (P_{open}) at 300 μM diC$_8$-PI(4,5)P_2 was 0.73±0.072 (n=10; Table 2). The concentration dependence of diC$_8$-PI(4,5)P_2-activated channel P_{open} could be reasonably well fitted by a single-site Hill equation, with EC_{50} of 120.3±32.43 μM and Hill slope (nH) of 2.08±0.348 (n=10) (Fig. 4, dashed line, and Table 2). This EC_{50} value is not significantly different from that obtained previously for homomeric Kv7.2

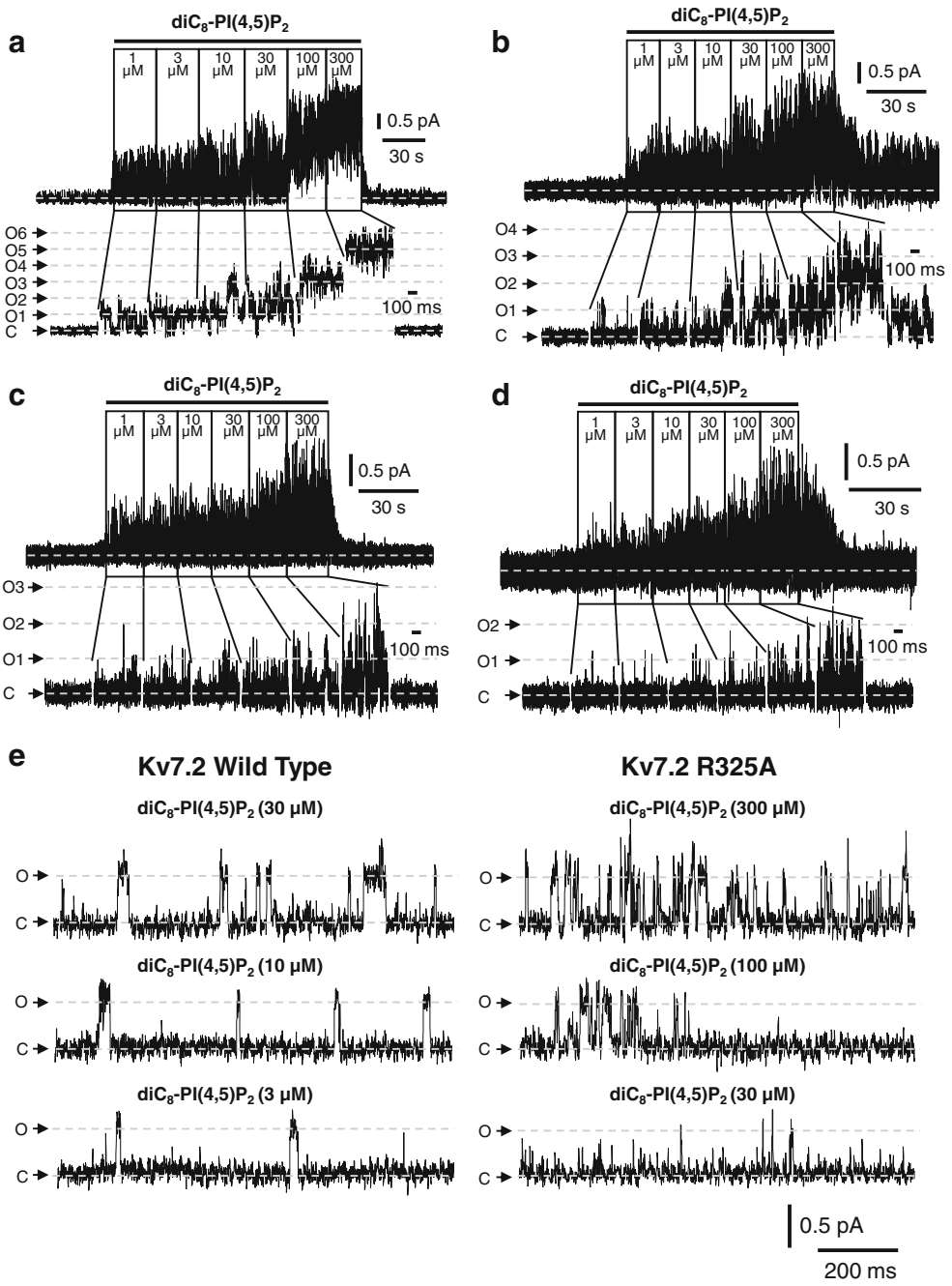

Fig. 3 Responses of wild-type and mutant Kv7.2 channel in excised inside-out patches to fast application of incremental concentrations of diC$_8$-PI(4,5)P_2 to the inside face of the patch. **a**–**d** Exemplar records of channel currents at 0 mV patch potential from cells transfected to express: **a** Wild-type Kv7.2, **b** Kv7.2 (K327A), **c** Kv7.2 (R325A), and **d** Kv7.2 (R325A/K327A). *Upper traces*: contracted time base; *lower traces*: expanded time base. *C* = closed channel current level; O1 to O*n* = current levels for 1 to *n* channels. **e** Further expanded records showing Kv7.2 (wild type) and Kv7.2 (R325A) activity recorded at comparable mean values for P_{open} (see Table 3)

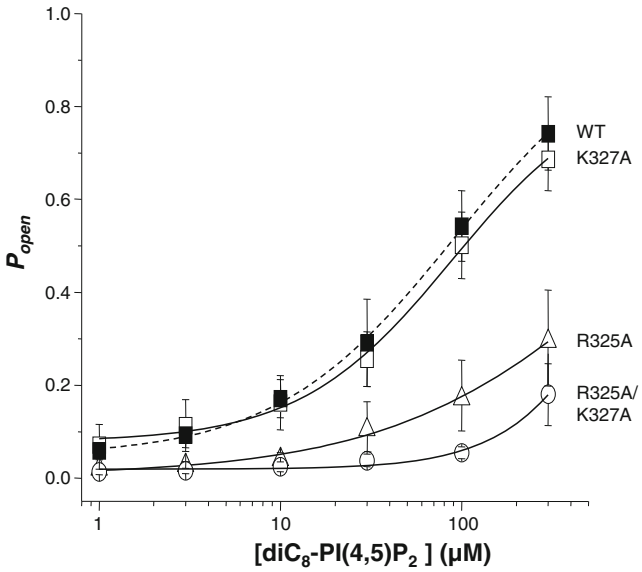

Fig. 4 Mean values±SEM (*bars*) for channel open probability P_{open} plotted against diC$_8$-PI(4,5)P$_2$ concentration (in micromolar from eight to ten patches for each type of channel (see Table 3 for mean data). Curves are unconstrained least-squares plots of a single-site Hill equation (Eq. (3) in 'Methods' section). Mean values for the parameters used are given in Table 2

channels expressed in these cells (76.2±19.9 μM [20]), though the present Hill slope appears rather steeper.

The mutated channel Kv7.2 (K327A) showed a virtually identical response to diC$_8$-PI(4,5)P$_2$ (Figs. 3b and 4), with maximum observed P_{open} at 300 μM of 0.69±0.067, EC_{50} 114.6±20.55 μM, and nH 1.06±0.111 (Table 2). P_{open} and EC_{50} values were not significantly different from those for wild-type channels. In contrast, the single mutant R325A (Fig. 3c) and the double-mutant R325A/K327A (Fig. 3d) produced a striking reduction in the sensitivity of the channels to diC$_8$-PI(4,5)P$_2$: P_{open} at 300 μM diC$_8$-PI(4,5)P$_2$ was reduced ~60 % for Kv7.2 (R325A) to 0.29±0.11 and for the double-mutant R325A/K327A by ~76 % to 0.18±0.067, while extrapolated EC_{50} values for diC$_8$-PI(4,5)P$_2$ were both shifted ~eightfold from wild type, to 0.98 mM (Fig. 4 and Table 2). These changes were not accompanied by any material change in single-channel current amplitudes, which remained generally within the range 0.50–0.55 pA (Table 2) as reported previously [20]. However, for similar values of P_{open} (Table 3), openings of the mutated channels did appear to be briefer (Fig. 3e), though we were unable to obtain a sufficient run of single-channel activity to construct full open-closed time distributions.

Discussion

These experiments indicate that the PI(4,5)P$_2$-sensing site previously identified in the proximal region of the C-terminal of Kv7.1 [22] is partly conserved in Kv7.2 and is crucially required in intact form for the normal activation of these channels by PI(4,5)P$_2$. Thus, mutation of arginine-325 (R325) in Kv7.2 (corresponding to R360 in Kv7.1) to the neutral amino acid alanine reduced the maximum Kv7.2 current by 60 %. This can be attributed primarily to a large reduction in the sensitivity of the channels to PI(4,5)P$_2$ because the EC_{50} for activation of the individual Kv7.2 channels by diC$_8$-PI(4,5)P$_2$ was raised about eightfold, from ~120 μM for the wild-type Kv7.2 channel to an extrapolated value near 1 mM, for the Kv7.2 (R325A) mutant. [The maximum observed P_{open} at 300 μM PI(4,5)P$_2$ was ~0.3 on average; since we could not test higher PI(4,5)P$_2$ concentrations, we cannot exclude an additional reduction in maximum open probability, see further below].

One difference from the Kv7.1 site is that the K327A mutation in Kv7.2 did not, by itself, significantly affect either channel sensitivity to PI(4,5)P$_2$ or macroscopic current amplitude, in contrast to the equivalent mutation (K362A) in Kv7.1 [22] (though it did preserve the effect of the R325A mutation in the double-mutant R325A/K327A). In addition, Zhang et al. [25] have previously reported that a mutation of the adjacent histidine-328 (Kv7.2 (H328C)) produced a threefold reduction in channel diC$_8$-PI(4,5)P$_2$ sensitivity when incorporated into Kv7.2/7.3 heteromers (equivalent to a near tenfold reduction for a Kv7.2 (H328C) homomer). Thus, this proximal Kv7.2 PI(4,5)P$_2$-sensing region appears to comprise (minimally) the two residues R325 and/H328.

Another difference from Kv7.1 concerns the effect of the mutations on channel voltage gating. The principal effect of PI(4,5)P$_2$ on the cardiac delayed rectifier Kv7.1/KCNE1 current is to increase its sensitivity to membrane depolarization, rather

Table 3 Effect of increasing concentrations of diC$_8$-PI(4,5)P$_2$ on P_{open} of wild-type and mutated Kv7.2 channels recorded in excised inside-out membrane patches: mean data

[diC$_8$-PI(4,5)P$_2$]	1 μM	3 μM	10 μM	30 μM	100 μM	300 μM
Kv7.2 WT (n=10)	0.088±0.032	0.108±0.048	0.163±0.056	0.292±0.094	0.452±0.087	0.727±0.072
K327A (n=10)	0.071±0.045	0.113±0.056	0.162±0.058	0.256±0.059	0.501±0.072	0.686±0.067
R325A (n=8)	0.020±0.007	0.027±0.009	0.040±0.015	0.104±0.060	0.171±0.083*	0.294±0.110**
R325A/K327A (n=8)	0.013±0.006	0.016±0.006	0.0024±0.011*	0.037±0.013*	0.055±0.013**	0.180±0.067***

*P<0.04, **P<0.004, ***P<0.001, significantly different from the wild type Kv7.2

than control the absolute current amplitude [14]. Thus, the R360A mutation in Kv7.1 shifted the activation curve for Kv7.1/KCNE1 by +44 mV [22]. In contrast, no significant shift in the conductance–voltage curve occurred with the equivalent R325A mutation of Kv7.2 (Fig. 2c and Table 1). However, the response of Kv7.1 channels to $PI(4,5)P_2$ is highly dependent on a tight association with KCNE1 [13]. Hence, and in accordance with our results on Kv7.2, the Kv7.1 (R360A) mutant produced only a minimal (+5 mV) shift of the activation curve for the Kv7.1 homomer in the *absence* of KCNE1 [2]. The present results also are in accord with previous observations that (for instance) the reduction in Kv7.2/7.3 (M) current produced by agonists that reduce membrane $PI(4,5)P_2$ is not accompanied by a change in the current's voltage sensitivity [1, 9, 15].

Previously, using mutational analysis combined with homology modelling and phosphoinositide docking simulations, a more distal Kv7.2 C-terminal domain in the linker between the A- and B-helices (see Fig. 1) containing the basic amino acid cluster K452/R459/R461 has been identified as forming a plausible binding site for $PI(4,5)P_2$ [10]. This suggestion was partly confirmed by a reduction in phosphoinositide binding to a Kv7.2 C-terminus fusion protein containing the triple mutant Kv7.2 (K452E/R459E/R461E) when compared with that of a wild-type fusion protein [21]. One possibility therefore is that $PI(4,5)P_2$ can bind to both the A-B linker site and the more proximal site containing R325A in Kv7.2 (as previously shown for the latter for Kv7.1 channels [22]). Alternatively, perhaps the proximal domain is more involved in the associated conformational change leading to channel opening (i.e. the 'gating' of the $PI(4,5)P_2$-activated channel), such that mutations of residues R325 and H328 reduce the stability of the activated channel. We cannot exclude this because we were unable to apply sufficient diC_8-$PI(4,5)P_2$ to directly measure the maximum open probability; and indeed some support for an effect on gating might be adduced from the apparently briefer channel openings noted for the Kv7.2 (R325A) channels (Fig. 3e). However, ligand binding and gating are intimately connected and effects of mutations on the two can be very difficult to distinguish from the channel response to an activating ligand [4]. Thus, in previous experiments on the response of heteromeric Kv7.2/7.3 channels to diC_8-$PI(4,5)P_2$, the effects of inserting the triple A-B linker–residue mutation in the Kv7.3 subunit [10] on this response could be better interpreted in terms of a change in the equilibrium gating constants than in the binding constants [20][1]. Further, structural evidence for a close coupling between $PI(4,5)P_2$ binding and K^+ channel conformational change has been adduced for Kir channel proteins [8, 24]. Notwithstanding, and importantly, even if the R325A mutation did affect gating, its action was specific to the effect of diC_8-$PI(4,5)P_2$ since the parameters for channel voltage gating were not altered.

Irrespective of the precise interpretation, the present and previous [25] results clearly show that the proximal C-terminal residues R325 and H328 play a major role in mediating the response of Kv7.2 channels to $PI(4,5)P_2$. Further, since they are conserved among all Kv7 channels, it seems reasonable to suggest that they might form part of an essential structural component required for the activation of this channel family by membrane phosphoinositides. Structures of Kir channels complexed with $PI(4,5)P_2$ have already shown the critical involvement of juxta-membrane residues in the response of this channel family to phosphoinositides [8, 24]. If our suggestions for the Kv7 family are confirmed, this raises the possibility of a universal involvement of conserved juxta-membrane domains in ion channel regulation by $PI(4,5)P_2$.

Acknowledgments This work was supported by grants 085419 from the Wellcome Trust and RG/10/10/28447 from the British Heart Foundation. We thank Ms. Sirikamol Srismith for help in preparing mutated Kv7.2 cDNAs.

[1] This kinetic scheme was developed for heteromultimeric Kv7.2/7.3 channels in which the two species of subunit have different sensitivities to $PI(4,5)P_2$. We could not apply it to the present observations because (a) data sets were insufficient to determine differences in microscopic constants and (b) we have no evidence to show that the same scheme applies to homomeric channels.

References

1. Adams PR, Brown DA, Constanti A (1982) Pharmacological inhibition of the M-current. J Physiol 332:223–262
2. Boulet IR, Labro AJ, Raes AL, Snyders DJ (2007) Role of the S6 C-terminus in KCNQ1 channel gating. J Physiol 585:325–337
3. Brown DA, Passmore GM (2009) Neural KCNQ (Kv7) channels. Br J Pharmacol 156:1185–1195
4. Colquhoun D (1998) Binding, gating, affinity and efficacy. Br J Pharmacol 125:923–947
5. Delmas P, Brown DA (2005) Pathways modulating neural KCNQ/M (Kv7) potassium channels. Nat Revs Neurosci 6:850–862
6. Gamper N, Shapiro MS (2007) Regulation of ion transport proteins by membrane phosphoinositides. Nat Revs Neurosci 8:921–934
7. Greenwood IA, Ohya S (2009) New tricks for old dogs: KCNQ expression and role in smooth muscle. Br J Pharmacol 156:1196–1203
8. Hansen SB, Tao X, Mackinnon R (2011) Structural basis of PIP2 activation of the classical inward rectifier K^+ channel Kir2.2. Nature 477:495–498
9. Hernandez CC, Falkenburger B, Shapiro MS (2009) Affinity for phosphatidylinositol 4,5-bisphosphate determines muscarinic agonist sensitivity of Kv7 K+ channels. J Gen Physiol 134:437–448
10. Hernandez CC, Zaika O, Shapiro MS (2008) A carboxy-terminal inter-helix linker as the site of phosphatidylinositol 4,5-bisphosphate action on Kv7 (M-type) K+ channels. J Gen Physiol 132:361–381
11. Jentsch TJ (2000) Neuronal KCNQ potassium channels: physiology and role in disease. Nat Rev Neurosci 1:21–30

12. Li Y, Gamper N, Hilgemann DW, Shapiro MS (2005) Regulation of Kv7 (KCNQ) K+ channel open probability by phosphatidylinositol 4,5-bisphosphate. J Neurosci 25:9825–9835
13. Li Y, Zaydman MA, Wu D, Shi J, Guan M, Virgin-Downey B, Cui J (2011) KCNE1 enhances phosphatidylinositol 4,5-bisphosphate (PIP2) sensitivity of IKs to modulate channel activity. Proc Natl Acad Sci U S A 108:9095–9100
14. Loussouarn G, Park KH, Bellocq C, Baro I, Charpentier F, Escande D (2003) Phosphatidylinositol-4,5-bisphosphate, PIP2, controls KCNQ1/KCNE1 voltage-gated potassium channels: a functional homology between voltage-gated and inward rectifier K+ channels. EMBO J 22:5412–5421
15. Marrion NV (1997) Control of M-current. Ann Rev Physiol 59:483–504
16. Park KH, Piron J, Dahimene S, Mérot J, Baró I, Escande D, Loussouarn G (2005) Impaired KCNQ1-KCNE1 and phosphatidylinositol-4,5-bisphosphate interaction underlies the long QT syndrome. Circ Res 96:730–739
17. Robbins J (2001) KCNQ potassium channels: physiology, pathophysiology, and pharmacology. Pharmacol Ther 90:1–19
18. Selyanko AA, Hadley JK, Wood IC, Abogadie FC, Jentsch TJ, Brown DA (2000) Inhibition of KCNQ1-4 potassium channels expressed in mammalian cells via M1 muscarinic acetylcholine receptors. J Physiol 522:349–355
19. Suh BC, Inoue T, Meyer T, Hille B (2006) Rapid chemically induced changes of PtdIns(4,5)P2 gate KCNQ ion channels. Science 314:1454–1457
20. Telezhkin V, Brown DA, Gibb AJ (2012) Distinct subunit contributions to the activation of M-type potassium channels by PI(4,5)P_2 J. Gen Physiol 140:41–53
21. Telezhkin V, Reilly JM, Thomas AM, Tinker A, Brown DA (2012) Structural requirements of membrane phospholipids for M-type potassium channel activation and binding. J Biol Chem 287:10001–10012
22. Thomas AM, Harmer SC, Khambra T, Tinker A (2011) Characterization of a binding site for anionic phospholipids on KCNQ1. J Biol Chem 286:2088–2100
23. Wang HS, Pan Z, Shi W, Brown BS, Wymore RS, Cohen IS, Dixon JE, McKinnon D (1998) KCNQ2 and KCNQ3 potassium channel subunits: molecular correlates of the M-channel. Science 282:1890–1893
24. Whorton MR, MacKinnon R (2011) Crystal structure of the mammalian GIRK2 K+ channel and gating regulation by G proteins, PIP2, and sodium. Cell 147:199–208
25. Zhang H, Craciun LC, Mirshahi T, Rohacs T, Lopes CM, Jin T, Logothetis DE (2003) PIP(2) activates KCNQ channels, and its hydrolysis underlies receptor-mediated inhibition of M currents. Neuron 37:963–975